

EVALUATING THE MASS OF ACTINIDES IN THE WASTE PACKAGES BY PHOTOFISSION USING MONTE CARLO N-PARTICLE EXTENDED CODE

M.N. Nasrabadi^{a,*}, M.R. Abdi^b, M. Mousavi^b

^a*Department of Nuclear Engineering, Faculty of Advanced Sciences & Technologies,
University of Isfahan, Isfahan, 81746-73441, Iran*

^b*Department of Physics, University of Isfahan, Isfahan, Iran
E-mail: mnnasrabadi@ast.ui.ac.ir*

INTRODUCTION

Once extracted from mine, nuclear materials pass through complex technical routes before exiting the last nuclear installation. Depending on the type of the equipment in the route, some radioactive materials enter the package. These waste packages have to be collected and maintained under controlled conditions for management and waste materials engineering. There are several technologies working at different stages of the nuclear fuel cycle in order to prevent contamination. However, for safety and economic reasons, controlling the waste materials requires determination of the main steps in the nuclear fuel cycle. To do so, non-destructive methods are usually applied because they are less expensive for the analysis of the waste materials compared to destructive methods [1]. In this study, the mass of actinides in waste packages was determined using photofission and MCNPX code. Using photons of high energy enables us to induce photofission reactions on the fissile nuclei present in the wastes. The measurement of the delayed neutrons emitted by fission products allows us to quantify the actinides present in the wastes. The accuracy of the method can be deeply improved by carrying out a tomography, i.e. computing the three-dimensional spatial distribution of the actinide mass inside the nuclear waste package. Since high-energy photons are used, this method seems to be well adapted to inspect large concrete waste packages as well.

SUMMARY OF THEORY

The method is based on the detection of delayed neutrons emitted by fission products, which are created by the photofission of actinides. Delayed neutrons created by photofission are counted between each pulse of photons and may be divided into six precursors groups, each group being characterized by a half-life time, relative yield abundance, and special energy [2,3]. The mean number of neutrons emitted per fission depends on the actinide species [4]. The values for ^{238}U and ^{239}Pu are shown in Table 1.

Table 1. Half-lives and relative abundance yield of the six groups of delayed neutrons for ^{238}U and ^{239}Pu

Isotope	Group i th	$t_{1/2}(\text{Sec})$	β_i
^{238}U	1	56.2	1.98
	2	21.3	15.7
	3	5.50	17.5
	4	2.15	31.1
	5	0.70	17.7
	6	0.19	16.1
^{239}Pu	1	54.0	6.05
	2	20.6	20.6
	3	5.70	18.3
	4	1.94	29.5
	5	0.58	14.9
	6	0.20	10.6

Temporal evolution of delayed neutrons can be described as a sum of six exponentials. After n pulses, the number of detected neutrons, N_c , is given by Eq. (1)

$$N_c = \varepsilon_n f \sum_{i=1}^6 \frac{\beta_i}{\lambda_i} (1 - e^{-\lambda_i t_p}) (1 - e^{-\lambda_i t_d}) (1 - e^{-\lambda_i t_c}) \Omega_i(n) \quad (1)$$

Where

$$\Omega_i(n) = \frac{(n+1)(1-\omega_i) - (1-\omega_i^{n+1})}{(1-\omega_i)^2} \quad (2)$$

$$\omega_i = e^{-\lambda_i \tau} \quad (3)$$

Where ε_n is the neutron detection efficiency, β_i is defined as the fraction of delayed neutrons in the i th group, λ_i (sec^{-1}) is the decay constant of i th group, $t_p(\text{sec})$ is the pulse duration, $t_d(\text{sec})$ is the time before starting counting, $t_c(\text{sec})$ is the counting time between two pulses, n is the total number of pulses, τ is the period of pulses, f is the photofission rate during pulse in the sample. When the total time of measurement, $T_m = n\tau$, is greater than 10 minutes, Eq. (1) can be approximated with an error less than 2% to Eq. (4).

$$N_c \cong \varepsilon_n n f t_p \frac{\beta_i}{\tau} \quad (4)$$

The photofission rate, f , in the above equations is given by

$$f = \frac{mN_A}{M} \int_{E_0}^{E_{\max}} \phi(E) \sigma_f(E) dE \quad (5)$$

where m is the mass of actinide, M is the molar mass of actinide, N_A is the Avogadro's number, σ_f is the photofission cross-section (cm^2), $\phi(E)$ is the photon flux per energy, ($\text{photons cm}^{-2} \text{s}^{-1} \text{MeV}^{-1}$).

The Eq. (4) is often written as, $f = \alpha_f f_0 M$, where f_0 is photo fission rate per each gram of actinide (assuming that the sample is in a non-attenuating point) and α_f is attenuation factor. By defining total effective counting time $T_c = nt_c$ and occupancy rate of the accelerator $\theta_p = t_p/\tau$, then delayed neutrons counting rate can be expressed by as

$$S_{net} = \frac{N_s}{T_s} = \varepsilon_n \alpha_f f_0 m \theta_p \quad (6)$$

As shown by Eq. (6) this counting rate is proportional to the mass of actinide inside the waste package. The basic goal of this work is to evaluate ε_n and α_f , both of which strongly depend on the geometry and the matrix of the package. They can be evaluated by simulation or by calibration with a standard package [2]. One of the main components is the delayed neutrons emitted by the following reactions: $^{18}\text{O}(\gamma, p)^{17}\text{N} \rightarrow ^{17}\text{O} \rightarrow ^{16}\text{O} + n$. Since the threshold of this reaction is 15.9MeV, we decided to study packages at energy lower than or equal to 15 MeV [5]. Matrix composition plays a major role in the performance of the method as for all non-destructive methods. Its role appears in two steps. First, during induction, the matrix can attenuate the photon flux reaching the sample of actinide, decreasing the term α_f in Eq. (6). In the second step, the matrix can absorb the delayed neutrons, decreasing the term ε_n in the same equation. Having information about geometry, position and matrix of the sample is crucial for the accuracy of the method.

SIMULATIONS

In order to simulate waste packages, calculation and experiment are carried out using a strong nuclear transport code named MCNPX. The code includes photonuclear reactions. MCNPX is a general Monte Carlo transport codes that began at Los Alamos fifty years ago and extends the MCNP4c code to higher energies and more particle types. MCNPX is released with libraries for neutrons, photons, electrons, protons and photonuclear interactions. In addition, variance reduction schemes and new tallies have been created specific to the intermediate and high energy physics [6].

MEASUREMENTS ON A LARGE CONCRETE PACKAGE

The set-up of waste package model is arranged by two coaxial cylinders, and one channel was used to put samples of nuclear materials at different positions. The diameter and the height of outer cylinder are 1.05m and 1.17m respectively. The diameter and the height of inner cylinder are 0.85m and 1.07m respectively. Around the waste package there are seven detectors for counting of delayed neutrons emitted by fission products. Fig. 1 shows the results of the simulated model of the waste package by MCNPX code. Table 2 gives the composition of the outer and inner cylinders.

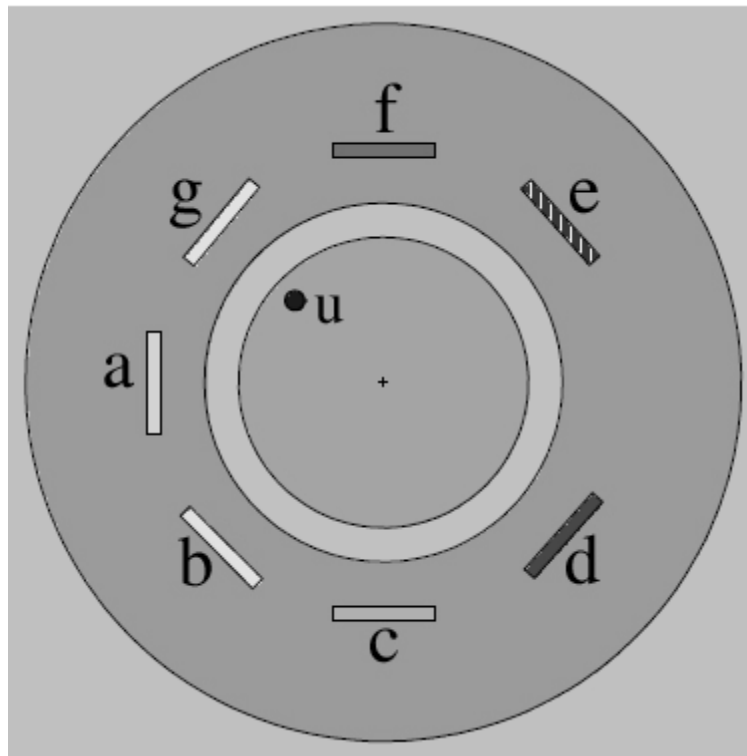


Fig. 1 Scheme of the concrete waste package

Table 2. Matrix composition of the inner and the outer cylinders [2]

Inner cylinder		Outer cylinder	
Element	Relative weight (%)	Element	Relative weight (%)
C	42.14	C	41.40
Fe	18.00	Cl	28.40
Cl	14.20	O	24.70
O	12.35	H	05.50
H	06.31		
Cr	04.50		
Ni	02.50		

Different amounts of %20 enrichment uranium (^{235}U 20 %, ^{238}U 80 %) are placed in these channels. We simulated the photon induction experiments by means of the MCNPX code. In experiment, the detection of delayed neutrons emitted by fission products were detected by seven detectors placed around of waste packages. Fig. 2 shows a linear relationship between the flux of neutrons and the changes in the amount of enriched uranium placed in waste package. Using this figure we will be able to estimate the weight of actinide mass in the waste packages. The background count is carried out by the net neutron counting.

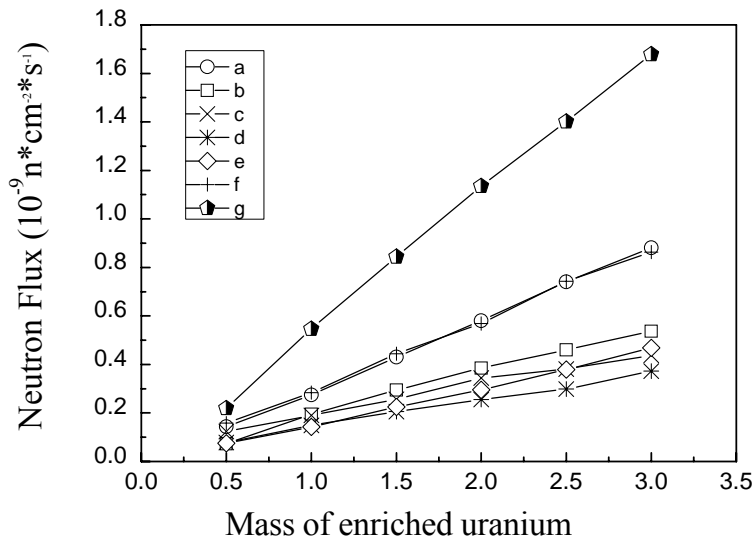


Figure 2 Neutron flux versus the mass change of U with 20% enrichment

In order to improve the results, we carried out the experiments with various energies of incident gamma rays. However, the best results obtained for energy levels near the peak of photonuclear reactions cross section, were better than the results for the photons with 14MeV energy. Then ^{239}Pu was put as the next sample in the waste package at various points in front of detectors *a*, *b*, *g* and between them. Fig. 3 shows the profile of neutron flux for different detectors.

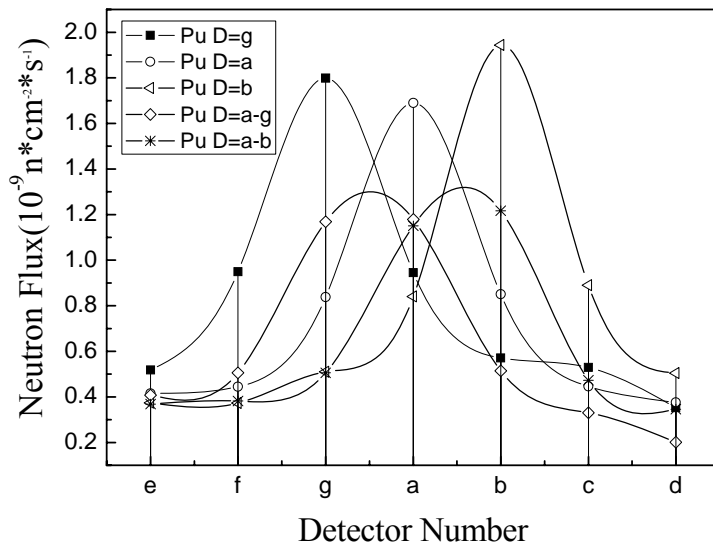


Figure 3 Neutron flux based on detector numbers for Pu

As it can be seen detector *g* is the closest detector to the actinide sample and therefore the best results were obtained for this detector. From the figure it is also possible to estimate the form, the type and the location of actinide sample inside the waste packages. Repeating this essay for %20 uranium and comparing the diagrams with those of ^{239}Pu and ^{238}U allows us to determine the type of actinide in waste packages (Fig. 4).

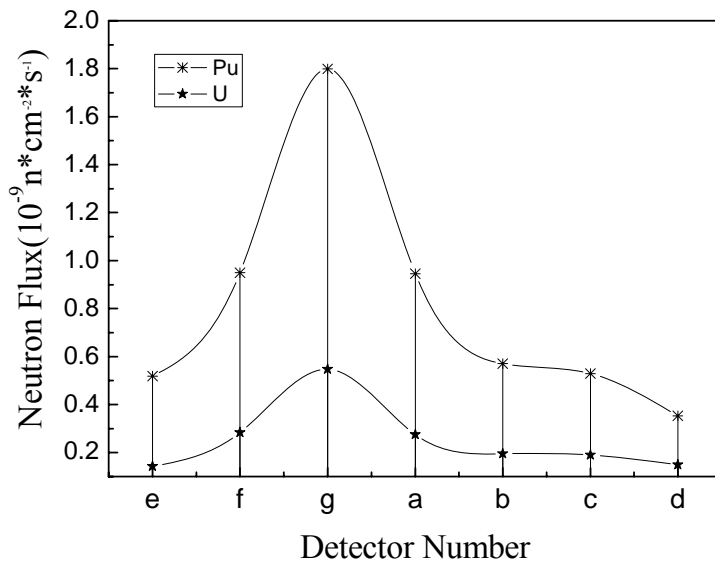


Figure 4 Neutron flux based on detector numbers for Pu and U

CONCLUSION

In this work, we obtained a linear relationship for each detector after plotting the neutron flux against changing the mass of actinide in the simulated samples (Fig. 4). Using this linear correlation it is possible to determine the mass of actinides in the nuclear waste packages which is of crucial importance. Also by changing the position of actinide samples we obtained neutron fluxes for detectors. Using these points and neutron fluxes a plane is obtained which can be used for determination of the precise location of actinide samples.

REFERENCES

- M. Gmar, F. Jeanneau, F. Laine, B. Poumarede. (2006) *Nucl. Instr. and Meth. A* 562, 1089–1092.
- M. Gmar, F. Jeanneau, F. Laine, H. Makil, B. Poumarede, F. Tola. (2005) *Appl. Rad and Isot.* 63 613–619.
- R.W. Waldo, R.A. Karam, R.A. Meyer. (1981) *Phys. Rev. C.* 23 1113–1127.
- J.T. Caldwell, E.J. Dowdy. (1975) *Nucl. Sci. Eng.* 56, 179–187.
- N. Saurel, J.M. Capdevila, N. Huot, M. Gmar. (2005) *Nucl. Instr. and Meth.*, A 550 691–699.
- Ut-Battelle, Llc (2002) *MCNPX User's Manual*, Version 2.4.0, Los Alamos National Laboratory, LA-CP-02-408.